CFTR is required for zinc-mediated antibacterial defense in human macrophages

Kaustav das Gupta, James Curson, Abdullah Tarique, Ronan Kapetanovic, Mark Schembri, Emmanuelle Fantino, Peter Sly, Matthew Sweet

PNAS RESEARCH ARTICLE | IMMUNOLOGY AND INFLAMMATION

CFTR is required for zinc-mediated antibacterial defense in human macrophages

Kaustav Das Gupta[a,b,1], James E. B. Curson[a,b,1], Abdullah A. Tarique[b,c], Ronan Kapetanovic[d,e], Mark A. Schembri[a,b,f], Emmanuelle Fantino[b,c], Peter D. Sly[b,c], and Matthew J. Sweet[a,b,2]

Edited by Katherine Fitzgerald, University of Massachusetts Medical School, Worcester, MA; received September 19, 2023; accepted December 22, 2023

Cystic fibrosis transmembrane conductance regulator (CFTR) is an anion transporter required for epithelial homeostasis in the lung and other organs, with *CFTR* mutations leading to the autosomal recessive genetic disease CF. Apart from excessive mucus accumulation and dysregulated inflammation in the airways, people with CF (pwCF) exhibit defective innate immune responses and are susceptible to bacterial respiratory pathogens such as *Pseudomonas aeruginosa*. Here, we investigated the role of CFTR in macrophage antimicrobial responses, including the zinc toxicity response that is used by these innate immune cells against intracellular bacteria. Using both pharmacological approaches, as well as cells derived from pwCF, we show that CFTR is required for uptake and clearance of pathogenic *Escherichia coli* by CSF-1-derived primary human macrophages. CFTR was also required for *E. coli*-induced zinc accumulation and zinc vesicle formation in these cells, and *E. coli* residing in macrophages exhibited reduced zinc stress in the absence of CFTR function. Accordingly, CFTR was essential for reducing the intramacrophage survival of a zinc-sensitive *E. coli* mutant compared to wild-type *E. coli*. Ectopic expression of the zinc transporter SLC30A1 or treatment with exogenous zinc was sufficient to restore antimicrobial responses against *E. coli* in human macrophages. Zinc supplementation also restored bacterial killing in GM-CSF-derived primary human macrophages responding to *P. aeruginosa*, used as an in vitro macrophage model relevant to CF. Thus, restoration of the zinc toxicity response could be pursued as a therapeutic strategy to restore innate immune function and effective host defense in pwCF.

antimicrobial response | cystic fibrosis | CFTR | macrophages | zinc

Cystic fibrosis (CF) is an autosomal recessive disorder caused by mutations in the CF transmembrane conductance regulator gene (*CFTR*) (1). As many as 2,000 different mutations in *CFTR* have been reported, with approximately 150 of these known to cause disease (2). CFTR is a member of the ATP-binding cassette (ABC) family of proteins (3), functioning primarily as an apical anionic channel for chloride and bicarbonate ions (4). Mutations in *CFTR* can reduce the number of functional channels and/or interfere with the overall function of the protein, affecting the normal flow of chloride and bicarbonate ions and water into and out of cells (2). Currently, all known *CFTR* mutations are classified into six categories, according to the type of phenotypic manifestation (5). The most common *CFTR* mutation is the deletion of phenylalanine 508 (ΔF508), with this mutation occurring in approximately 70% of people with CF (pwCF) (6, 7). The ΔF508 mutation results in destabilized CFTR protein folding due to altered stability of the nucleotide-binding domain, leading to its proteasomal degradation and reduced cell surface residence time (8).

CFTR is ubiquitously expressed, but its expression is particularly high in lung epithelial tissues (9). Although CF is primarily an airways disease disrupting normal lung function, it also manifests in other organs such as the pancreas and gastrointestinal tract (2). *CFTR* mutations result in mucus accumulation in the lungs, narrowing of the airway lumen, obstructive pulmonary disease, and bronchiectasis. This creates an environment conducive to inflammation and recurring infections caused by *Pseudomonas aeruginosa*, *Staphylococcus aureus,* and other pathogens. *P. aeruginosa* infections in pwCF are associated with a decline in lung function, exaggerated lung inflammation, and increased mortality (10, 11). Nontuberculous mycobacterium infections, especially those caused by *Mycobacterium abscessus*, are also common in CF, accounting for approximately 3 to 20% of infections in pwCF (12).

In addition to epithelial cells, CFTR is also expressed in immune cells, including tissue-resident macrophages, monocytes, neutrophils, and lymphocytes (13). Macrophages and neutrophils are key innate immune leukocytes that infiltrate compromised lungs of pwCF and contribute to CF pathology (14). Macrophages harboring mutations in *CFTR*

Significance

Mutations in the cystic fibrosis transmembrane conductance regulator gene (*CFTR*) cause CF, a disease characterized by aberrant lung function, dysregulated innate immunity, and susceptibility to infections. Combination drugs such as elexacaftor–tezacaftor–ivacaftor (ETI) restore lung function in most people with CF (pwCF), but there is little evidence that they correct innate immune defense. We show that CFTR is required for the macrophage zinc toxicity antibacterial response and that manipulating zinc availability can restore bacterial killing in CFTR-defective macrophages. Significance lies in identification of a link between CFTR and the macrophage zinc toxicity response and of approaches that could be used to restore innate immune antimicrobial defense in pwCF. Our findings may lead to strategies to reduce infections in pwCF.

Author contributions: K.D.G., A.A.T., R.K., P.D.S., and M.J.S. designed research; K.D.G., J.E.B.C., A.A.T., and R.K. performed research; A.A.T., M.A.S., E.F., P.D.S., and M.J.S. contributed new reagents/analytic tools; K.D.G., J.E.B.C., A.A.T., and M.J.S. analyzed data; K.D.G., J.E.B.C., A.A.T., R.K., M.A.S., E.F., P.D.S., and M.J.S. edited the paper; K.D.G., R.K., E.F., P.D.S., and M.J.S. supervised the research; R.K., P.D.S., and M.J.S. acquired funding; and K.D.G., J.E.B.C., and M.J.S. wrote the paper.

The authors declare no competing interest.

This article is a PNAS Direct Submission.

[1]K.D.G. and J.E.B.C. contributed equally to this work.

[2]To whom correspondence may be addressed. Email: m.sweet@imb.uq.edu.au.

This article contains supporting information online at https://www.pnas.org/lookup/suppl/doi:10.1073/pnas.2315190121/-/DCSupplemental.

Published February 16, 2024.

have a proinflammatory phenotype, as well as impaired host defense responses (15). High neutrophil elastase activity in bronchoalveolar fluids of infants is associated with early bronchiectasis in children with CF (16), and neutrophil extracellular traps increase the viscosity of airway secretions, promoting biofilm formation (17). Macrophages from pwCF also exhibit defects that likely contribute to disease manifestations. These include increased secretion of proinflammatory cytokines such as IL-1β, IL-6, and TNF (15, 18, 19), as well as impaired antimicrobial responses such as phagocytosis (20) and phagolysosome acidification (21). Additionally, monocyte-derived macrophages from pwCF are defective in alternative activation/M2 polarization, with reduced surface expression of CD209 and IL-13Rα1 (22). Agents that restore CFTR function, such as ivacaftor and lumacaftor, can correct various defects in monocytes from pwCF, including dysregulated inflammatory responses (23) and impaired antimicrobial defense (24, 25). Despite the overall success of CFTR modulators in improving clinical outcomes, many pwCF, particularly those harboring a G551D mutation in *CFTR*, often report reemergence of symptoms after treatment cessation (26). Furthermore, the prevalence of multiantibiotic-resistant bacterial pathogens calls for the development of new strategies to combat persistent infections in pwCF.

In addition to well-characterized antimicrobial responses, such as generation of reactive oxygen and nitrogen species, antimicrobial peptides, lysosomal acidification, and nutrient deprivation, metal ion toxicity has emerged as a key host defense pathway in macrophages (27). Studies with copper- and zinc-sensitive mutants of various bacterial pathogens have highlighted the role of metal ion trafficking in direct antimicrobial targeting of intracellular pathogens. For example, human macrophages subject *Mycobacterium tuberculosis* to zinc-mediated toxicity (28), while a similar response is employed by neutrophils against *Streptococcus pyogenes* (29). Furthermore, some bacterial pathogens, such as *Salmonella enterica* serovar Typhimurium (*S. Typhimurium*) (30) and uropathogenic *Escherichia coli* (UPEC) (31), can evade macrophage-mediated zinc poisoning of intracellular bacteria. CFTR may be relevant to the innate immune zinc toxicity response since this ABC transporter is required for both chloride and bicarbonate anion transport, processes that are also linked to zinc trafficking. The SLC39A family of zinc importers deliver zinc into the cytoplasm from either the extracellular environment or luminal compartments within cells. These transporters are symporters that transport both metal ions and bicarbonate (32), the latter of which is also transported by CFTR (33). Conversely, the SLC30A family of zinc exporters that transport zinc from the cytoplasm to the extracellular space or luminal compartments in cells are thought to be antiporters that facilitate pH-driven zinc transport in exchange for H^+ (34–36), with phagosome acidification known to be defective in pwCF (37). Here, we investigate the role of CFTR in the macrophage zinc toxicity response, finding that this anion transporter is required for initiation of this antimicrobial response. Furthermore, we show that amplifying the zinc toxicity response in CFTR-inhibited macrophages enhances clearance of bacterial pathogens such as UPEC and *P. aeruginosa*. We thus establish boosting of metal ion toxicity as a potential means of overcoming defective host defense in pwCF.

Results

CFTR-inhibited Macrophages Are Defective in Phagocytosis and Killing of Intracellular *E. coli*. To begin to generate a molecular understanding of how CFTR contributes to host defense in macrophages, we assessed the effects of the small molecule CFTR inhibitor C172 (38) on macrophage responses to *E. coli*. Initial experiments assessed responses of primary human macrophages that had been differentiated from monocytes in the presence of C172 (to mimic the long-term defect that is apparent in CF). Consistent with a role for CFTR in endocytosis (22) and phagocytosis (39), C172 significantly reduced phagocytic uptake and/or acidification of fluorescently labeled *E. coli* by primary human macrophages (Fig. 1*A*). We next investigated this defect in phagocytosis using the UPEC ST131 reference strain EC958 (40). Uptake of UPEC, as assessed by intracellular bacterial loads at 20 min p.i. (Fig. 1*B*), was also significantly reduced. Consequently, intracellular bacterial loads were also reduced at 2 h and 8 h p.i. (*SI Appendix*, Fig. S1*A*). However, when quantifying intracellular UPEC survival relative to initial uptake, bacterial loads were substantially increased at 2 h and 8 h p.i. (Fig. 1 *C* and *D*). This is consistent with previous observations using *P. aeruginosa* (21, 41) and suggests that macrophage antimicrobial responses engaged after the initial uptake of bacteria require CFTR. To further examine this possibility and to avoid the complication of CFTR inhibition affecting phagocytosis, intramacrophage bacterial loads were next assessed when human monocyte-derived macrophages (HMDM) were first treated with C172 at 1 h p.i. with UPEC (Fig. 1*E*). In these experiments, intracellular bacterial loads were again increased, particularly at the later time point of 8 h p.i. (Fig. 1 *F* and *G* and *SI Appendix*, Fig. S1*B*), suggesting that CFTR contributes to antimicrobial responses in macrophages after bacterial uptake. We further validated these phenotypes using monocyte-derived macrophages from pwCF that harbor the ΔF508 mutation. Consistent with the CFTR inhibition data (Fig. 1 *A*–*G*), these macrophages were significantly impaired in both uptake and clearance of intracellular UPEC (Fig. 1 *H* and *I* and *SI Appendix*, Fig. S1*C*). CFTR deficiency thus compromises at least two aspects of antimicrobial defense, phagocytosis and direct killing of bacteria.

Macrophages employ several inducible antimicrobial responses to combat persistent intracellular infections, including nutrient starvation and metal ion toxicity (27). Of note, zinc toxicity has emerged as an important antimicrobial mechanism in macrophages, with this pathway being subverted by both UPEC and *Salmonella* (30, 31, 42). In *E. coli* and other Gram-negative bacteria, the transporter ZntA effluxes zinc when zinc concentrations reach cytotoxic levels, thus conferring zinc resistance (43, 44). High levels of environmental zinc up-regulate the expression of this transporter in UPEC (Fig. 2*A*), with this effect being selective to zinc versus other metal ions (31). The expression of this transporter is also elevated in *E. coli* within infected macrophages, consistent with engagement of the zinc toxicity response by these innate immune cells (31). Moreover, UPEC partly evades the macrophage zinc toxicity response, unlike the nonpathogenic *E. coli* K12 strain MG1655 (31). To investigate whether CFTR contributes to macrophage-mediated zinc toxicity against *E. coli*, we assessed *zntA* expression in the otherwise susceptible *E. coli* strain MG1655. In CFTR-inhibited macrophages, *zntA* mRNA levels were significantly lower than in vehicle-treated control macrophages (Fig. 2*B*), suggesting that the zinc toxicity response was impaired. A similar phenotype was apparent in macrophages from pwCF, where *zntA* mRNA levels of intramacrophage *E. coli* were lower than those in macrophages from healthy donors (HD) (Fig. 2*C*). Collectively, these data suggest that CFTR is required for optimal zinc trafficking in macrophages for deployment of the zinc toxicity response against intracellular bacteria.

CFTR Is Required for Bacteria-Inducible Zinc Accumulation in Human Macrophages. In response to TLR4 (Toll-like receptor 4) signaling or bacterial infection, macrophages accumulate intracellular zinc and mobilize this metal ion into vesicular

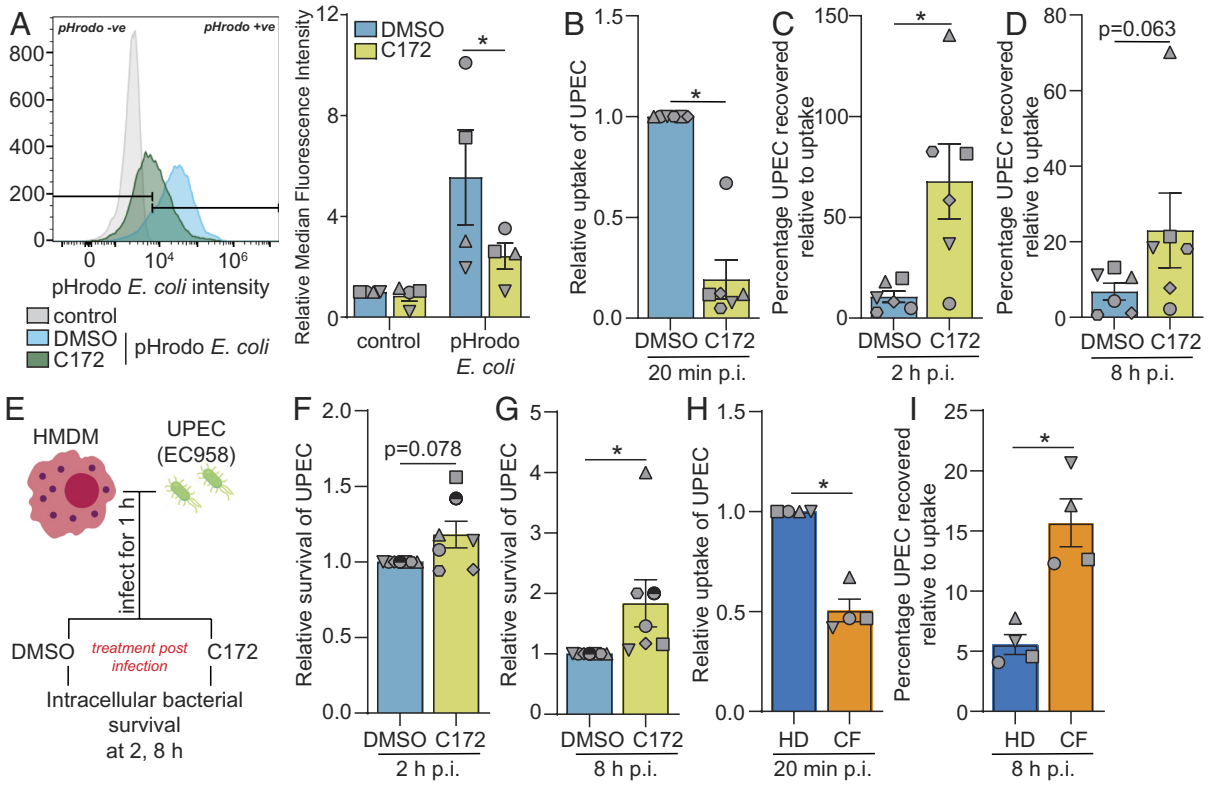

Fig. 1. CFTR is required for uptake and clearance of intracellular *E. coli* by human macrophages. (*A*) HMDM were differentiated with CSF-1 ± 10 μM C172 or vehicle dimethyl sulfoxide (DMSO) for 6 d, after which phagocytosis assays were performed using pHrodo *E. coli* and flow cytometry. Representative flow cytometry plot (*Left*) and quantified flow cytometry data normalized to the baseline DMSO control in each experiment (*Right*) (n = 4). (*B–D*) HMDM were differentiated with CSF-1 ± 10 μM C172 or vehicle (DMSO) for 6 d, after which they were infected with EC958 (UPEC) (MOI 100) for the indicated time points. Intracellular bacterial loads were quantified using gentamicin exclusion assays. Data in *B* are normalized to the DMSO control for each experiment, and data in *C* and *D* are presented relative to uptake for the relevant treatment in *B* (n = 6). (*E*) Schematic representation of the infection assay protocol used in *F* and *G*. (*F* and *G*) HMDM were infected with UPEC (MOI 100) for 1 h after which C172 (10 μM) or vehicle (DMSO) was added to the cells for the indicated time points. Intracellular bacterial loads were quantified using gentamicin exclusion assays. Data are normalized to the DMSO control for each experiment (n = 7). (*H* and *I*) HMDM from healthy donors (HD) or pwCF (CF) were differentiated with CSF-1 for 6 d and then infected with UPEC (MOI 100) for the indicated time points. Intracellular bacterial loads were quantified using gentamicin exclusion assays. Data in *H* are normalized to the HD for each experiment, and data in *I* are presented relative to bacterial uptake in *H* (n = 4). Data (mean ± SEM) are combined from at least four independent experiments (each using different donors). Statistical significance was assessed by two-way ANOVA (*A*) followed by Sidak's multiple comparison test or Wilcoxon test (*B–D* and *F–I*) (*$P < 0.05$).

structures that contain intracellular bacteria (31, 42). Since analysis of *zntA* expression in *E. coli* within macrophages implicated CFTR in the zinc toxicity response (Fig. 2), we next determined whether CFTR was required for *E. coli*-induced zinc accumulation in macrophages. Treatment with either bacterial lipopolysaccharide (LPS) or *E. coli* for 24 h increased levels of

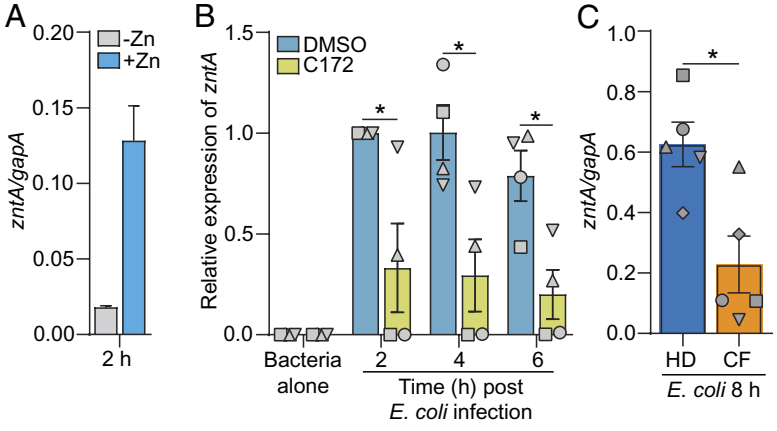

Fig. 2. CFTR is required for a zinc stress response in nonpathogenic *E. coli* within macrophages. (*A*) Nonpathogenic *E. coli* (strain MG1655) was grown in the presence of 500 μM $ZnSO_4$ for 2 h. Total RNA was extracted, and *zntA* mRNA levels were assessed using qPCR. Data are representative of two independent experiments. (*B*) HMDM were differentiated with CSF-1 ± 10 μM C172 or vehicle (DMSO) and infected with *E. coli* strain MG1655 (MOI 100) for the indicated time points, after which total RNA was extracted. Expression levels of *E. coli zntA* mRNA (relative to *gapA*) within HMDM versus bacterial alone were assessed using qPCR. Data are normalized to the 2 h DMSO infection control (n = 4). (*C*) Total RNA was extracted from healthy or CF HMDM and infected with *E. coli* (MOI 100) for 8 h. Expression levels of *E. coli zntA* mRNA (relative to *gapA*) within HMDM were assessed using qPCR (n = 5). Data (mean ± SEM) are combined from at least four independent experiments (each using different donors). Statistical significance was assessed using two-way ANOVA followed by Sidak's multiple comparison test (*B*) or Mann–Whitney test (*C*) (*$P < 0.05$).

exchangeable zinc in macrophages, as detected by FluoZin-3 staining (Fig. 3 *A*, *Left* and *SI Appendix*, Fig. S2 *A* and *B*), with this response being attenuated in CFTR-inhibited cells (Fig. 3 *A*, *Right*). Similarly, the *E. coli*-induced increase in FluoZin-3 staining did not occur in macrophages from pwCF (Fig. 3 *B* and *C*). To eliminate the possibility that the reduced intracellular zinc staining resulted from reduced uptake of bacteria (Fig. 1 *A*, *B*, and *H*), CFTR was inhibited pharmacologically with C172 after bacterial uptake. Even in this setting where intracellular bacterial loads were increased (Fig. 1 *F* and *G*), *E. coli*-induced zinc accumulation was significantly reduced (Fig. 3*D*). Total intracellular zinc levels were also quantified by ICP-OES (inductively coupled plasma optical emission spectroscopy) to provide a more direct measure of zinc accumulation. These experiments confirmed that infection with *E. coli* increased zinc levels within macrophages, with CFTR inhibition reducing this response (Fig. 3*E*).

Zinc trafficking is controlled by the SLC39A/ZIP family of zinc importers and the SLC30A/ZNT family of zinc exporters (45). TLR ligation and *E. coli* infection up-regulates *SLC30A1* expression in human macrophages, with this transporter being functionally linked to zinc vesicle formation and the zinc toxicity response (42). For example, ectopic expression of SLC30A1 in human monocyte-like THP-1 cells was sufficient to generate zinc-containing vesicles in macrophages in the absence of TLR activation (42). We found that CFTR inhibition attenuated *E. coli*-inducible *SLC30A1* mRNA expression in human macrophages (Fig. 3*F*). In contrast, there

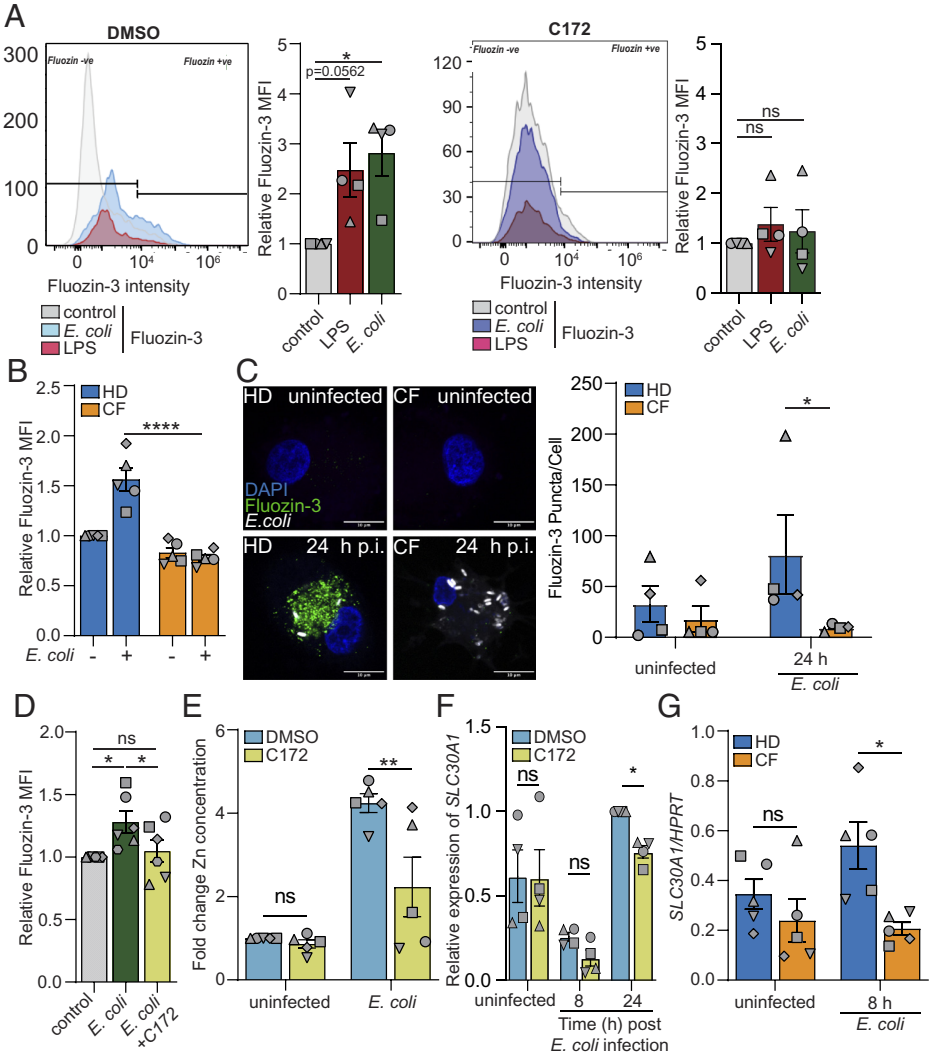

Fig. 3. CFTR is required for zinc accumulation in human macrophages. (*A*) HMDM were differentiated with CSF-1 ± 10 μM C172 or vehicle (DMSO) for 6 d, after which they were either stimulated with LPS (20 ng/mL) or infected with *E. coli* (MOI 100) for 24 h. Relative intracellular zinc levels were determined by FluoZin-3AM staining and flow cytometry (*Left*: DMSO control, *Right*: C172). Representative flow cytometry plots and quantified flow cytometry data normalized to the baseline control in each experiment are depicted (n = 4). (*B*) Monocytes from HD or pwCF (CF) were differentiated into HMDM with CSF-1 for 6 d, after which they were infected with *E. coli* (MOI 100) for 24 h. Relative intracellular zinc levels were determined by FluoZin-3AM staining and flow cytometry. Data are normalized to the HD control in each experiment (n = 5). (*C*) Monocytes from HD or pwCF (CF) were differentiated into HMDM with CSF-1 for 6 d, after which they were infected with *E. coli*-mCherry (MOI 100) for 24 h. Intracellular zinc-containing vesicles were visualized by immunofluorescence microscopy (FluoZin-3AM: green; *E. coli*-mCherry: white, DAPI: blue; scale bars: 10 μm), *Left*. The number of zinc-containing puncta per cell was quantified, *Right* (n = 4). (*D*) HMDM were infected with *E. coli* (MOI 100) for 1 h after which 10 μM C172 or vehicle (DMSO) was added to the cells for 24 h. Relative intracellular zinc levels were determined by FluoZin-3AM staining and flow cytometry. Data are normalized to the control in each experiment (n = 6). (*E*) HMDM were differentiated with CSF-1 ± 10 μM C172 or vehicle (DMSO) for 6 d, after which they were infected with *E. coli* (MOI 100) for 24 h. Absolute intracellular zinc levels were determined by ICP-OES. Data are normalized to the DMSO control in each experiment (n = 5). (*F* and *G*) Total RNA was extracted from HMDM differentiated ± 10 μM C172 or vehicle (DMSO) for 6 d (n = 4) (*F*) or from matched HD and pwCF (CF) (n = 5) (*G*) after infection with *E. coli* (MOI 100) for the indicated time points. Expression levels of *SLC30A1* mRNA were assessed using qPCR. Data in *F* are normalized to the DMSO control for 24 h *E. coli* infection. Data (mean ± SEM) are combined from at least four independent experiments (each using different donors). Statistical significance was assessed using the nonparametric Kruskal–Wallis test (*A*), Friedman's test (*D*), or two-way ANOVA (*B*, *C*, and *E*–*G*) followed by Sidak's multiple comparison test (ns, not significant; *$P < 0.05$; **$P < 0.01$; ****$P < 0.0001$).

was a clear trend toward elevated *TNF* mRNA levels (*SI Appendix*, Fig. S2*C*), consistent with the hyperinflammatory phenotype that is observed in pwCF (15, 18, 19). CFTR-dependent control of *SLC30A1* mRNA expression was more evident when examining macrophages from pwCF. Here, we observed that *SLC30A1* mRNA expression was significantly reduced in macrophages from pwCF infected with *E. coli* for 8 h, compared to healthy donor macrophages (Fig. 3*G*). The coordinated actions of SLC39A and SLC30A zinc transporters are likely to enable zinc mobilization for antimicrobial responses in macrophages (45). The requirement for CFTR in inducible *SLC30A1* mRNA expression is therefore consistent with impaired zinc accumulation in CFTR-inhibited macrophages.

CFTR Is Required for the Zinc Toxicity Response in Human Macrophages. Genetic deletion of *zntA* reduces the intracellular survival of *E. coli* within macrophages (31). If CFTR is required for zinc-mediated antimicrobial defense, the reduction in intramacrophage survival of Δ*zntA E. coli* should not occur in the absence of a functional CFTR. Indeed, although C172 impaired phagocytic uptake of both wild-type and Δ*zntA E. coli* as expected (Fig. 4*A*), C172 prevented the ~twofold reduction in intramacrophage survival of the Δ*zntA E. coli* at 8 h p.i. (Fig. 4*B*). In fact, there was a trend for increased intracellular loads of Δ*zntA E. coli*, compared to wild-type *E. coli*, in C172-treated cells. Specifically, the recovery of Δ*zntA E. coli* compared to wild-type *E. coli* in DMSO vehicle-treated HMDM at 8 h p.i. was 61%, compared to 156% recovered in C172-treated HMDM (means of five experiments). Similar findings were apparent in macrophages from pwCF. In these cells, initial uptake of both bacterial strains was again impaired compared to macrophages from HD (Fig. 4*C*). Furthermore, the ~twofold reduction in intramacrophage survival of Δ*zntA E. coli* that was observed in macrophages from HD did not occur in macrophages generated from pwCF (Fig. 4*D*). Here, the recovery of Δ*zntA E. coli* compared to wild-type *E. coli* in macrophages from HD at 8 h p.i. was 43%, compared to 96% in macrophages from pwCF (means of four experiments). Collectively, these data confirm that macrophages without a functional CFTR protein fail to deploy the zinc toxicity response against intracellular *E. coli*.

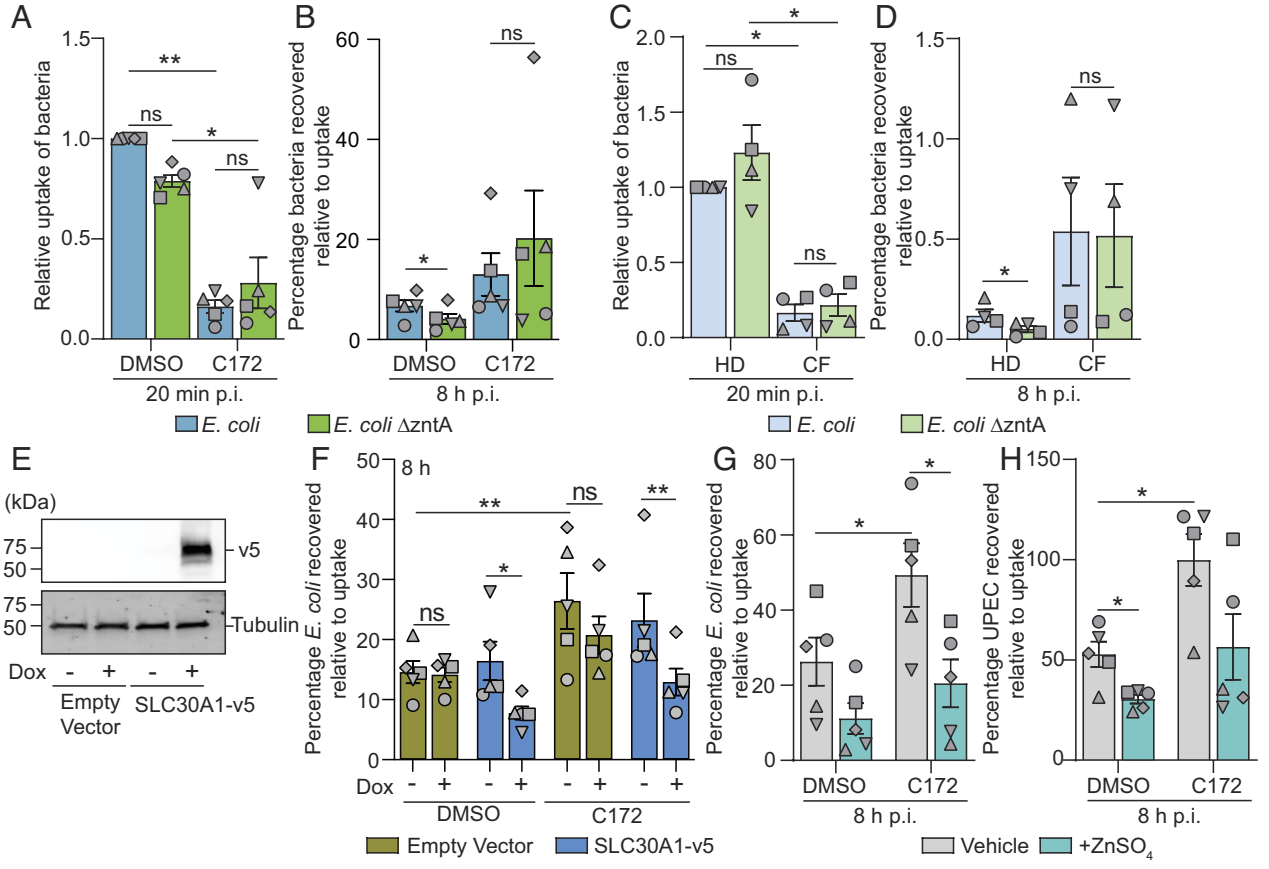

Fig. 4. CFTR is required for the macrophage zinc toxicity response, with ectopic SLC30A1 expression or zinc supplementation restoring host defense in macrophages with defective CFTR function. (*A* and *B*) HMDM were differentiated with CSF-1 ± 10 μM C172 or vehicle (DMSO) for 6 d, after which they were infected with *E. coli* or *E. coli* Δ*zntA* (MOI 100) for the indicated time points. Intracellular bacterial loads were quantified using gentamicin exclusion assays and expressed as percentage bacteria retrieved (*B*), relative to initial uptake (*A*) (n = 5). (*C* and *D*) Monocytes from HD or pwCF (CF) were differentiated into HMDM with CSF-1 for 6 d, after which they were infected with *E. coli* or *E. coli* Δ*zntA* (MOI 100) for the indicated time points. Intracellular bacterial loads were quantified using gentamicin exclusion assays and expressed as percentage bacteria retrieved (*D*) with respect to uptake (*C*) (n = 4). (*E* and *F*) PMA-differentiated THP-1 cells stably transduced with lentivirus expressing either empty vector or SLC30A1_V5 were treated ± doxycycline (Dox) for 24 h and then assessed for SLC30A1-V5 protein levels by anti-V5 immunoblots on cell lysates (*E*). Cells ± 24 h doxycycline treatment were infected with *E. coli* (MOI 100) for 8 h, after which intracellular bacterial loads were assessed using gentamicin exclusion assays (n = 5) (*F*). The immunoblots in *E* are representative of three independent experiments. (*G* and *H*) HMDM were differentiated with CSF-1 ± 10 μM C172 or vehicle (DMSO) for 6 d, after which they were treated with 200 μM of $ZnSO_4$ for 1 h and then infected with *E. coli* (*G*) or UPEC (*H*) (MOI 100) for 8 h. Intracellular bacterial loads were quantified using gentamicin exclusion assays and expressed as percentage bacteria retrieved with respect to uptake (n = 5). Data are combined from at least four independent experiments (each using different donors) in *A*–*D*, *G*, and *H* or five independent experiments in *F* and are expressed as mean ± SEM. Statistical significance was assessed using two-way ANOVA followed by Tukey's multiple comparison test (ns, not significant; **P* < 0.05; ***P* < 0.01).

The Defective Zinc Toxicity Response in Macrophages from pwCF Can Be overcome by Genetic Manipulation of This Pathway or Zinc Supplementation. We next investigated the possibility that artificial amplification of the zinc toxicity response in CFTR-inhibited macrophages might be able to overcome the defect in bacterial killing. We previously reported that doxycycline-inducible ectopic expression of the zinc exporter *SLC30A1* in THP-1 macrophages mobilizes zinc vesicles and enhances zinc toxicity against intracellular *E. coli* (42). Consistent with previous observations, ectopic expression of SLC30A1 in THP-1 cells using a doxycycline-inducible system (Fig. 4*E*) reduced intracellular loads of *E. coli* in these cells at 8 h p.i. (Fig. 4*F*) and 24 h p.i. (*SI Appendix*, Fig. S3*A*), whereas doxycycline did not affect bacterial loads in empty vector (EV) control cells at these time points. Interestingly, overexpressing SLC30A1 in CFTR-inhibited THP-1 cells eliminated the defect in antimicrobial responses of these macrophages, with these cells having similar intracellular bacterial loads to those with a functional CFTR. Our previous work also showed that exogenous zinc treatment facilitated intramacrophage clearance of *Salmonella*, which normally evades this pathway (30). Given that SLC30A1 overexpression overcame the CFTR-mediated defect in the macrophage zinc toxicity response and that zinc supplementation of macrophages enhanced clearance of intracellular bacteria (30), we predicted that exogenous zinc treatment of macrophages might also overcome this defect. Here, we found that concentrations of zinc that did not inhibit the growth of either nonpathogenic *E. coli* or pathogenic EC958 (*SI Appendix*, Fig. S3*B*) significantly improved the ability of CFTR-inhibited macrophages to reduce intracellular loads of both nonpathogenic and pathogenic *E. coli* (Fig. 4 *G* and *H* and *SI Appendix*, Fig. S3 *C* and *D*). Collectively, these data demonstrate a requirement for CFTR in the macrophage zinc toxicity response and suggest that artificial enhancement of this pathway may overcome defective innate immune defense in pwCF.

CFTR Is Required for the Antimicrobial Zinc Response against *P. aeruginosa* in GM-CSF-Derived Macrophages. Having established a role for CFTR in the macrophage zinc toxicity response, we next assessed the potential clinical significance of this using an in vitro model of lung infection. Alveolar macrophages are crucial in preserving lung function during pulmonary infections (46, 47). These resident tissue macrophages of the lung rely on GM-CSF for their development and function (48, 49). We therefore assessed the zinc toxicity response in GM-CSF-derived human macrophages responding to *P. aeruginosa*, a common and significant bacterial pathogen in pwCF (50). Consistent with our previous observations assessing *E. coli* uptake and killing by CSF-1-derived macrophages (Fig. 1 *A*–*D*), pharmacological inhibition of CFTR significantly impaired the ability of GM-CSF-derived macrophages to take up *P. aeruginosa* (Fig. 5*A* and *SI Appendix*, Fig. S4*A*) and to subsequently kill this pathogen (Fig. 5 *B* and *C* and *SI Appendix*, Fig. S4*A*). Similarly, GM-CSF-derived macrophages from pwCF were defective in *P. aeruginosa* uptake and killing (Fig. 5 *D* and *E* and *SI Appendix*, Fig. S4*B*). To uncouple the roles of CFTR in bacterial uptake versus the subsequent bacterial killing response, we next pharmacologically inhibited CFTR after initial *P. aeruginosa* uptake (Fig. 5*F*). In this setting, intracellular bacterial loads were elevated after CFTR inhibition, though some variability in macrophages from different donors was observed (Fig. 5 *G*–*I* and *SI Appendix*, Fig. S4*C*).

Effects of zinc on *P. aeruginosa* growth are complex. Zinc promotes *P. aeruginosa* growth and biofilm formation (51), but higher concentrations are growth inhibitory (52). Zinc also inhibits signaling pathways associated with *P. aeruginosa* virulence (53). We therefore assessed the effects of zinc in macrophage responses against *P. aeruginosa* infection. Here, we observed a trend toward increased zinc accumulation in GM-CSF-derived macrophages from HD after *P. aeruginosa* infection (Fig. 5*J*), although the effect was not as pronounced as was observed after *E. coli* challenge in CSF-1-derived macrophages (Fig. 3 *A* and *B*). In contrast, *P. aeruginosa* did not increase the zinc content of GM-CSF-derived macrophages from pwCF, as assessed by FluoZin-3 staining (Fig. 5*J*). The combination drug cocktail elexacaftor–tezacaftor–ivacaftor (ETI) corrects CFTR function and restores lung function in pwCF carrying the ΔF508 mutation (54). CFTR correction with ETI also reduces, but does not eliminate, infections caused by common bacterial pathogens such as *P. aeruginosa* in pwCF (55, 56). Here, we observed that ETI did not restore cellular zinc levels in GM-CSF-derived macrophages from pwCF after infection with *P. aeruginosa* (Fig. 5*J*). Similarly, ETI did not restore zinc vesicle formation in CSF-1-derived macrophages from pwCF, as assessed by FluoZin-3 staining and confocal microscopy (*SI Appendix*, Fig. S4*E*). Nonetheless, while exogenous zinc treatment did not increase the capacity of macrophages from pwCF to take up bacteria (Fig. 5*K*), it did significantly reduce *P. aeruginosa* loads within macrophages from both HD and pwCF (Fig. 5*L* and *SI Appendix*, Fig. S4*D*). Collectively, these data show that CFTR is required for the macrophage zinc toxicity response and that zinc supplementation can overcome the defect in host defense that is apparent in macrophages from pwCF.

Discussion

CF pathology is usually considered to arise from defects in the epithelium of the airways. However, cell-intrinsic defects in innate immune cells, particularly monocyte-derived macrophages, are also thought to contribute to the pathogenesis of this condition. Macrophages from pwCF display dysregulated metabolic activity, characterized by the excessive secretion of proinflammatory mediators that accelerate tissue damage, as well as impaired phagocytosis and attenuated antimicrobial ROS production (57). Novel strategies that correct macrophage dysfunctions in pwCF may therefore lead to new treatment options for these people. Direct poisoning of bacteria by zinc and other metal ions is used by macrophages as an antimicrobial response against several bacterial pathogens (28, 30, 31, 45, 58). In this study, we show that the macrophage zinc toxicity response against intracellular *E. coli* requires CFTR, as evidenced by defective zinc accumulation (Fig. 3 *A, B*, and *E* and *SI Appendix*, Fig. S2), zinc vesicle formation (Fig. 3*C*), zinc stress in intracellular *E. coli* (Fig. 2 *B* and *C*), inducible expression of the zinc exporter SLC30A1 that can promote the zinc toxicity response (42) (Fig. 3 *F* and *G*), and killing of a zinc-sensitive *E. coli* mutant (Fig. 4 *A*–*D*) in cells in which CFTR is either inhibited (C172) or inactive (pwCF). Interestingly, treatment with ETI did not restore intracellular zinc levels in GM-CSF-derived macrophages from pwCF (Fig. 5*J*) or zinc vesicle formation in CSF-1-derived macrophages from pwCF (*SI Appendix*, Fig. S4*E*). This suggests that CFTR-correcting drugs may not restore the defective macrophage zinc-mediated antimicrobial response in pwCF, a concept that clearly warrants further investigation. In contrast, either overexpression of the zinc transporter SLC30A1 that can promote intracellular zinc vesicle formation and the zinc toxicity response (42) (Fig. 4*F*) or treatment with exogenous zinc (Figs. 4 *G* and *H* and 5 *K* and *L*) reduced intracellular bacterial loads in CFTR-defective macrophages. This implies that the requirement for CFTR in the zinc toxicity response can be overcome under these experimental conditions.

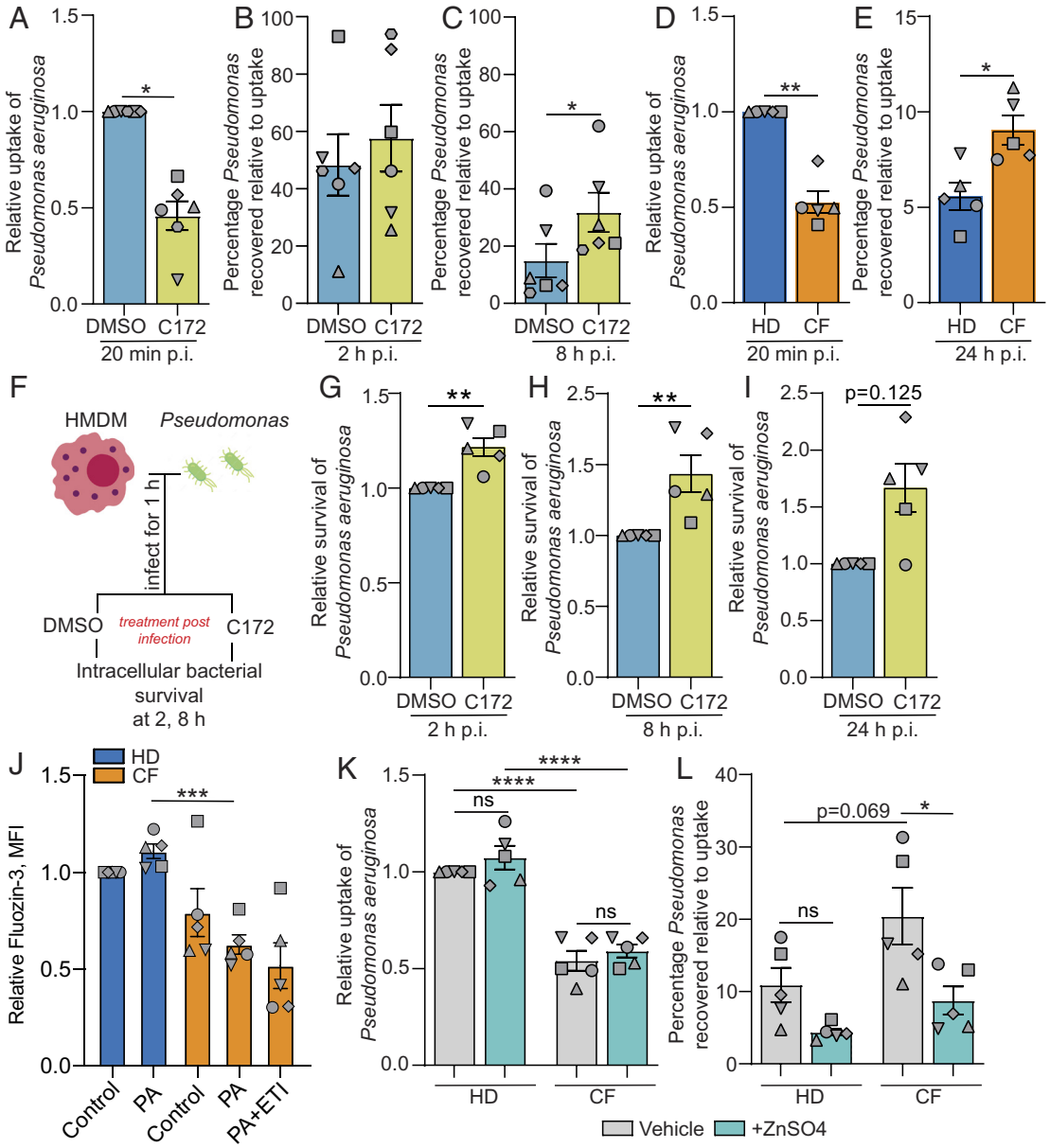

Fig. 5. CFTR contributes to the antimicrobial zinc response against *P. aeruginosa* in GM-CSF-derived macrophages. (*A–C*) HMDM were differentiated with GM-CSF ± 10 μM C172 or vehicle (DMSO) for 6 d, after which they were infected with *P. aeruginosa* (PA14) (MOI 5) for the indicated time points. Intracellular bacterial loads were quantified using gentamicin exclusion assays. Data in *A* are normalized to the DMSO control for each experiment, and data in *B* and *C* are presented relative to uptake for the relevant treatment in *A* (n = 6). (*D* and *E*) HMDM from HD or pwCF (CF) were differentiated with GM-CSF for 6 d, after which they were infected with PA14 (MOI 5) for the indicated time points. Intracellular bacterial loads were quantified using gentamicin exclusion assays. Data in *D* are normalized to the healthy donor (HD) control for each experiment, and data in *E* are presented relative to uptake for the relevant treatment in *D* (n = 5). (*F*) Schematic representation of the infection assay used in *G–I*. (*G–I*) GM-CSF-derived HMDM were infected with PA14 (MOI 5) for 1 h after which C172 (10 μM) was added to the cells for the indicated time points. Intracellular bacterial loads were quantified using gentamicin exclusion assays. Data are normalized to the DMSO control for each experiment (n = 5). (*J*) Monocytes from HD or pwCF (CF) were differentiated into HMDM with GM-CSF for 6 d. CF monocytes were also differentiated ± elexacaftor 3 μM/tezacaftor 18 μM/ivacaftor 1 μM (ETI). Cells were then infected with PA14 (MOI 5) for 24 h after which relative intracellular zinc levels were determined by FluoZin-3AM staining and flow cytometry. Data are normalized to the HD control for each experiment (n = 5). (*K* and *L*) GM-CSF-derived HMDM from HD or pwCF (CF) were treated with 200 μM of $ZnSO_4$ for 1 h prior to infection with PA14 (MOI 5) for 20 min or 24 h. Intracellular bacterial loads were quantified using gentamicin exclusion assays. Data in *K* are normalized to the healthy donor (HD) control for each experiment, and data in *L* are presented relative to uptake for the relevant treatment in *K* (n = 5). Data (mean ± SEM) are combined from at least four independent experiments (each using different donors). Statistical significance was assessed using the Wilcoxon test (*A–C* and *G–I*), Mann–Whitney test (*D* and *E*), or two-way ANOVA (*J–L*) followed by Tukey's multiple comparison test (ns, not significant; **P* < 0.05; ***P* < 0.01; ****P* < 0.001; *****P* < 0.0001).

Clinical, epidemiological, and experimental studies have linked reduced zinc availability with the development and/or progression of several respiratory diseases, including chronic obstructive pulmonary disease, idiopathic pulmonary fibrosis, COVID-19, and CF (59). This may reflect key roles for zinc in promoting host defense (60), dampening inflammation (60), and even in regulating tissue architecture in the lung. For example, rats placed on a zinc-deficient diet had reduced bronchial cilia length, with this defect being reversed by zinc supplementation (61). Dysregulated zinc levels in both adults and children with CF have been reported, with zinc generally being low in the blood and high in the sputum (62–65). It is possible that such effects are a consequence of the condition since systemic inflammatory responses trigger a decrease in circulating zinc levels (hypozincemia) (66) and since infection by respiratory pathogens can promote zinc accumulation in the lung (67). However, it is also possible that dysregulation in zinc

levels in CF relates to an essential role for CFTR in zinc trafficking, a concept that is supported by observations made in the current study. Another group also showed that CFTR deficiency leads to the generation of a spliced isoform of the zinc importer ZIP2, resulting in zinc deficiency in airway epithelial cells and MUC5AC hypersecretion (68). Studies on the zinc exporter SLC30A1 are also suggestive of a role for CFTR on zinc trafficking. Ectopic expression of SLC30A1 in human THP-1 macrophage-like cells facilitated zinc vesicle formation, a zinc stress response in intracellular *E. coli*, and bacterial clearance from cells (42). That study revealed that SLC30A1, while primarily being localized to the plasma membrane of human macrophages, also marked compartments containing zinc-stressed bacteria. This suggests that SLC30A1 may directly deliver zinc to phagosomes containing internalized bacteria. SLC30A family members are thought to be antiporters that export zinc in exchange for protons (34, 35), so the acidified environment of the phagolysosome is likely to facilitate SLC30A1-mediated delivery of zinc into these compartments. This may be relevant to CF, where lysosomal acidification is impaired (37). Given the above model, defects in phagolysosome acidification would be predicted to interfere with the inducible zinc toxicity response in macrophages, consistent with our findings here. Another interesting possibility comes from studies in *Drosophila melanogaster*, where it was discovered that chloride ions form part of zinc storage complexes in granules within cells of the Malpighian tubule (69). If the same is true in macrophages, this may shed some light on how CFTR enables the antimicrobial zinc toxicity response to be generated. For example, chloride ion availability in the phagolysosome may be a critical determinant of engagement of this antimicrobial pathway. Another possibility is that defective zinc accumulation in macrophages from pwCF could dysregulate other immune-relevant metals. For example, zinc influences circulating levels of iron (70) and it has been shown that macrophages from pwCF are defective in iron sequestration (71). That study also showed that conditioned media from macrophages derived from pwCF supported *Pseudomonas* biofilm formation, with a defect in sequestration of extracellular iron proposed to contribute to this effect. Interestingly however, CFTR correctors restored iron accumulation in macrophages from pwCF (71), which contrasts with our findings examining the effects of ETI on zinc accumulation in the current study. Whatever the precise mechanisms, the evidence above suggests that defects in CFTR perturb zinc trafficking and that this dysregulation may actively contribute to CF-associated pathology, such as mucus hypersecretion and defective host defense.

Apart from its antimicrobial functions, zinc is also an important regulator of inflammatory responses. Zinc deficiency exacerbates inflammatory responses, including in the airways (72). Consequently, oral zinc supplementation therapies have been trialed in CF, with variable results (73–75). While this regime reduced proinflammatory IL-6 and IL-8 levels in the plasma of CF patients (74), another study reported no improvements in lung function or in reducing *P. aeruginosa* colonization in pediatric patients with CF (75). Oral administration of zinc can also have undesirable side effects on airway epithelial cells such as bronchial hyperresponsiveness, olfactory loss, sensitization to common aeroallergens, and exacerbation of allergies (76–79), which might impair efficacy of chemical modulators in the treatment of CF. Thus, zinc supplementation for restoration of antimicrobial defense in CF, while effective in reducing intracellular bacterial loads in CFTR-defective macrophages in vitro (Figs. 4 *G* and *H* and 5 *K* and *L*), may have limitations as a therapeutic approach in pwCF. Zinc ionophores, such as PBT2 that synergizes with antibiotics to combat both Gram-positive and Gram-negative bacterial infections (80, 81), might be considered as one approach to selectively boost zinc-mediated host defense in this setting. Enhancement of molecular pathways that engage the zinc toxicity response, for example amplifying SLC30A1 expression and/or function, may be another.

Several clinically approved drugs can correct the defective anionic conductance of the CFTR channel, with this transforming the lives of many pwCF (82–84). The ETI combination therapy is perhaps the most successful drug to date for treating CF, with clinical studies confirming its efficacy in pwCF carrying the ΔF508 mutation (83, 85). While clinical studies using ETI report decreased sputum density of *Pseudomonas* and *Staphylococcus*, along with reduced inflammatory markers in the lung (86, 87), other studies reported that this combinational treatment was ineffective (88, 89). Macrophages from pwCF treated with ETI exhibited enhanced CFTR expression and localization in addition to increased phagocytic uptake and killing of ingested bacteria and efferocytosis of apoptotic neutrophils (90). However, some other key macrophage functions affected by CFTR mutations were largely unaffected by ETI treatment (90). It should be noted that this lack of efficacy is mainly associated with pwCF harboring the G551D mutation, which accounts for ~3% of the total population of pwCF (91). However, macrophages derived from pwCF used in this study had at least one ΔF508 mutation. It would be interesting to see whether the beneficial effects of zinc observed in our studies extend to pwCF carrying non- ΔF508 mutations. Future studies should also address how severe the effects of different CFTR mutations are on the macrophage zinc toxicity response, including in the context of cells from pwCF who are heterozygous for the ΔF508 mutation. Cells derived from pwCF in the current study were mainly homozygous for ΔF508 (*SI Appendix*, Table S1), so this was not addressed here.

In summary, in this study, we reveal an unexpected link between CFTR and zinc-mediated antimicrobial defense in macrophages. The findings reported here are significant for two key reasons. First, the precise molecular mechanisms underpinning the macrophage zinc toxicity pathway are not well understood. The identification of a requirement for CFTR in engaging this response now provides broad avenues to better understand this pathway, for example, the role of chloride ion transport and/or H^+ exchange. Second, defects in the macrophage zinc toxicity response may contribute to compromised host defense and susceptibility to bacterial infections that are characteristic of CF. Strategies aimed at restoring the zinc toxicity pathway in macrophages may complement ETI and similar therapies that restore CFTR function in the majority of pwCF, but that do not completely overcome CF-related pathology.

Materials and Methods

Ethics Statement. Human peripheral blood was collected from HD and pwCF following informed consent, after which mononuclear cells were isolated. Monocytes from pwCF were either homozygous (12 out of 18) or heterozygous (6 out of 18) for the ΔF508 mutation (*SI Appendix*, Table S1). All experiments that used these cells were approved by The University of Queensland Institutional Human Research Ethics Committee (2013/HE001519, 2022/HE002118, and 2020001275/HREC/20/QCHQ/64229).

Chemicals and Reagents. The CFTR inhibitor 4-[[4-oxo-2-thioxo-3-[3-(trifluoromethyl)phenyl]-5-thiazolidinylidene]methyl]-benzoic acid (C172, Cayman Chemical) was dissolved in DMSO and used at a final concentration of 10 μM (22). The TLR4 agonist LPS from *S. enterica* serotype Minnesota was purchased from Sigma-Aldrich (Cat – L2137) and dissolved in RPMI media (Gibco). The concentrations used for the three drugs that constitute Trikafta were elexacaftor 3 μM, tezacaftor 18 μM, and ivacaftor 1 μM (ETI) (92).

Bacterial Culture. Bacterial strains were cultured at 37 °C on solid or liquid Luria-Bertani (LB) medium. Nonpathogenic *E. coli* K12 strain MG1655 (93), a zinc-sensitive *zntA* mutant of MG1655 (31), MG1655_mCherry that constitutively expresses mCherry (94), a representative strain of the globally disseminated

multidrug-resistant ST131 clone isolated from the urine of a patient with a urinary tract infection (EC958) (40, 95), and a clinically relevant reference strain of *P. aeruginosa* (PA14) (96), were used in this study. Overnight cultures of *E. coli* MG1655 and PA14 were grown under shaking conditions, while EC958 cultures were grown statically to induce type I fimbriae production, as previously described (95). Before infection, bacteria were washed twice and resuspended in macrophage infection medium (described below). Optical density at 600 nm (OD_{600}) was measured, and bacterial suspensions were diluted to $OD_{600} = 0.6$, which corresponds to ~10^9 cfu/mL for *E. coli* and *P. aeruginosa*. Bacterial growth ± zinc sulfate (Sigma-Aldrich) was assessed by monitoring OD_{600} using a POLARstar Omega plate reader (BMG Labtech) at 30-min intervals.

Mammalian Cell Culture. $CD14^+$ human monocytes derived from either HD or pwCF were purified from buffy coats provided by the Australian Red Cross Blood Service or from pwCF, respectively. HMDM were generated by culturing monocytes for 7 d in Iscove's Modified Dulbecco's Medium (IMDM, Gibco) containing 10% fetal calf serum (FCS, Gibco), 50 U/mL penicillin (Life Technologies), 50 μg/mL streptomycin (Life Technologies), 2 mM L-glutamine and either recombinant human CSF-1 (150 ng/mL) (The University of Queensland Protein Expression Facility) or recombinant human GM-CSF (50 ng/mL) (Miltenyi Biotec). Where indicated, the CFTR inhibitor C172 (Cayman Chemical) was added daily to differentiating monocytes to mimic chronic CFTR deficiency, as occurs in CF. For experiments involving CFTR correctors/potentiators, ETI was added to monocytes on days 0, 3, and 7 of differentiation. ETI was also added to the cell culture media for the duration of the infection assays. The doxycycline-inducible system for expression of the zinc transporter SLC30A1 with a C-terminal V5 epitope tag in THP-1 cells has been described (42). THP-1 cells lentivirally transduced with either empty vector (EV) or SLC30A1-V5 were cultured in RPMI-1640 media (Gibco) supplemented with 10% FCS (Gibco), 50 U/mL penicillin (Life Technologies), 50 μg/mL streptomycin (Life Technologies), 2 mM GlutaMax (Life Technologies), 1% 4-(2-hydroxyethyl)-1-piperazine ethanesulfonic acid (HEPES, Thermo Fischer Scientific), and 1% sodium pyruvate (Gibco). Cells were differentiated using phorbol 12-myristate 13-acetate (PMA) (30 ng/mL) (Sigma-Aldrich) for 48 h ± C172. SLC30A1-V5 protein expression was induced by treating cells with 100 ng/mL doxycycline (Cat – D9891, Sigma-Aldrich) for 24 h, as described below. For all infection assays (see below), cells were cultured in IMDM supplemented with 10% FCS. All cells were cultured at 37 °C and 5% CO_2, unless otherwise indicated.

Quantification of Phagocytic Uptake of Bacteria. Phagocytic uptake of bacteria was assessed using pHrodo Green *E. coli* bioparticles (Thermo Fisher Scientific), as previously described (94). Briefly, primary macrophages (5×10^5 cells) were treated with 100 μg of pHrodo bacterial particles for 1 h, after which bacterial uptake was assessed by flow cytometry (Cytoflex, Beckman Coulter). Alternatively, primary macrophages were spinfected with *E. coli* MG1655, EC958, or PA14 for 5 min at 500 g at 35 °C, using a multiplicity of infection (MOI) of 100 (for *E. coli*) or 5 (PA14). The cells were then rested for 5 min before removing extracellular bacteria with gentamicin (200 μg/mL) (Thermo Fisher Scientific). Bacterial uptake at 20 min post-infection (p.i.) was assessed by counting colony forming units (CFU), as described below.

In Vitro Infection Assays. In vitro bacterial infections of primary macrophages and cell lines were carried out as previously described (97). Briefly, 1 to 4×10^5 cells were seeded overnight in antibiotic-free IMDM media. An MOI of 100 was used for both *E. coli* MG1655 and EC958, whereas *P. aeruginosa* infections were carried out using MOI of 5. At 1 h p.i., cells were washed and maintained in medium containing 200 μg/mL gentamicin to exclude any extracellular bacteria for 1 h, after which cells were washed with media again and maintained in medium containing 20 μg/mL gentamicin (Thermo Fisher Scientific). At appropriate time points, cells were washed twice with phosphate buffered saline (PBS) before being lysed in PBS containing 0.01% Triton X100. Diluted lysates were plated onto LB agar and incubated overnight at 37 °C. Numbers of colonies were counted to determine intracellular CFU. At all time points where the media were replaced during infection assays, 10 μM C172 or 200 μM $ZnSO_4$ was readded to the media for relevant treatment groups.

Gene Expression Analyses. Total RNA (bacterial and human) was extracted using RNA purification kits (Qiagen), as per the manufacturer's instructions. Genomic DNA was removed using an on-column DNAse digestion (Qiagen). RNA was reverse transcribed to cDNA using Superscript III (Invitrogen) and oligo dT (for mammalian targets) or random hexamers (for bacterial genes). Levels of specific mRNAs were quantified by qPCR using SyBR Green-PCR mix (Invitrogen) in the Applied Biosystems Viia 7 RT-PCR system. Appropriate negative controls with no Superscript III were included for all experiments. Data were expressed relative to the housekeeping gene hypoxanthine phosphoribosyltransferase (*HPRT*, human) or *gapA* (*E. coli* housekeeping gene) using the ΔCt method (98). Primers used for RT-qPCR are listed in *SI Appendix*, Table S2.

Estimation of Total Cellular Zinc Levels By Flow Cytometry. The zinc content of human macrophages post-LPS stimulation or bacterial infection was indirectly assessed using staining with 5 μM FluoZin-3AM (Thermo Fisher Scientific), as previously described (30). Briefly, primary macrophages (2×10^5 cells) were either treated with LPS (20 ng/mL) or infected with indicated bacterial species for 24 h, as described above. Post-treatment, cells were washed with PBS and stained for 30 min with FluoZin-3AM. The cells were washed again with PBS and then harvested in ice-cold PBS containing 0.1% sodium azide and 25 mM ethylenediamine tetraacetic acid (EDTA). Flow cytometric analysis was performed using a CytoFLEX flow cytometer (Beckman).

Quantification of Total Cellular Zinc Levels by ICP-OES. The zinc content of human macrophages was directly measured by ICP-OES, as previously described (31). Briefly, 5×10^6 HMDM were infected with MG1655 (MOI 100) for 24 h, as described above. At 24 h p.i., cells were washed twice with Hanks' balanced salt solution, lysed in 5 mL of lysis solution (0.1% sodium dodecyl sulfate in MilliQ water), and placed into preweighed 10-mL plastic tubes (School of Earth and Environmental Sciences, The University of Queensland, Australia). Triple distilled HNO_3 was then added to acidify the sample to 2%. The sample was then made up to a total volume of 10 mL with MilliQ water. Samples were analyzed using an Optima 8300 DV ICPOES spectrometer (Perkin Elmer, USA). Freshly prepared calibration standards were used to estimate intramacrophage zinc concentrations (with two or three spectral lines measured as a quality control). The overall concentration of zinc within a macrophage was approximated based on the zinc concentration within 1 million macrophages lysed in 1 mL of lysis buffer (as determined by ICP-OES).

Confocal Microscopy and Zinc Vesicle Quantification. Cells (2×10^5) were plated on coverslips in a 24-well plate in complete IMDM media and left to adhere overnight. Cells were infected using fluorescent *E. coli* MG1655_mCherry as described in figure legends before being washed twice with PBS and fixed with 4% PFA (Sigma-Aldrich) for 20 min. Cells were washed 3 times with PBS before being stained for intracellular zinc with 5 μM FluoZin-3AM and nuclear DNA with 1 μg/mL DAPI (Life Technologies). Coverslips were washed 3 times with PBS before being mounted on slides using IMBiol mounting media, and slides were viewed using a Zeiss Axiovert 200 Upright Microscope stand with LSM 710 Meta Confocal Scanner and spectral detection with 63× magnification (Zeiss). Images were processed with FIJI (ImageJ), and Zinc puncta were quantified by counting FluoZin-3AM maxima per cell (minimum 50 cells per condition) using the "Find maxima" function.

Immunoblotting. Whole cell lysates were prepared in radioimmunoprecipitation assay (RIPA) buffer, containing a cocktail of 1× protease inhibitors (Roche) and 1× PhosSTOP phosphatase inhibitors (Sigma-Aldrich). Immunoblotting was performed by electrophoresing equal amounts of protein through precast BOLT gels (Invitrogen), followed by turbo transfer onto nitrocellulose membranes at 25V for 9 min (Bio-Rad). Membranes were blocked using 5% bovine serum albumin (BSA) diluted in Tris-buffered saline containing 0.05% Tween 20 followed by probing with either anti-V5 (CAT: MCA1360, Bio-Rad) or rhodamine-conjugated anti-Tubulin (CAT: 12004165, Bio-Rad). Proteins were visualized using Clarity ECL (Bio-Rad) or through detection of fluorescent antibodies using a Chemidoc (Bio-Rad).

Statistical Analyses. Where statistical analyses were performed, data were combined from three or more independent experiments, with each experiment (n) designated by a different symbol. In the case of experiments on primary human macrophages, each experiment used cells from different donors and is represented by a different symbol. Statistical analyses were performed using Prism 9 software (Graph-Pad), with data combined from at least three independent experiments (taking averages from replicates within each experiment) and error bars indicating the SEM. Statistical analyses that used nonparametric tests included the Mann–Whitney *t* test (unpaired), Wilcoxon *t* test (paired), Kruskal–Wallis test and

Friedman's test. For experiments analyzing matched samples or data, repeated-measures ANOVA was performed. For datasets with two or more variables, a two-way ANOVA was performed followed by Tukey's or Sidak's multiple comparison test. Statistical tests used for individual experiments are described in the figure legends. Differences with confidence values of 95% ($P < 0.05$) were considered statistically significant.

Data, Materials, and Software Availability. All study data are included in the article and/or *SI Appendix*.

ACKNOWLEDGMENTS. This work was supported by National Health and Medical Research Council of Australia Investigator grants to M.J.S. and P.D.S. (APP1194406 and APP1193840, respectively), a Rebecca L. Cooper grant to R.K. (#021765), and an Australian Infectious Diseases Research Centre Basic-Clinical Seed Grant to M.J.S. and P.D.S. Microscopy was performed at the Institute for Molecular Bioscience Microscopy Facility which was established with the support of the Australian Cancer Research Foundation and incorporates the Dynamic Imaging, Cancer Biology Imaging and Cancer Ultrastructure and Function Facilities. We thank the pwCF who participated in this study, the Australian Red Cross Lifeblood for providing buffy coats for the isolation of human monocytes, and Protein Expression Facility at The University of Queensland for the generation of recombinant human CSF-1.

Author affiliations: [a]Institute for Molecular Bioscience, The University of Queensland, Brisbane, QLD 4072, Australia; [b]Australian Infectious Diseases Research Centre, The University of Queensland, Brisbane, QLD 4072, Australia; [c]Child Health Research Centre, The University of Queensland, Brisbane, QLD 4101, Australia; [d]Friedrich Miescher Institute for Biomedical Research, Basel, BS 4058, Switzerland; [e]Institut national de recherche pour l'agriculture, l'alimentation et l'environnement (INRAE), Université de Tours, Infectiologie et Santé Publique (ISP), Nouzilly 37380, France; and [f]School of Chemistry and Molecular Biosciences, The University of Queensland, Brisbane, QLD 4072, Australia

1. M. Shteinberg, I. J. Haq, D. Polineni, J. C. Davies, Cystic fibrosis. *The Lancet* **397**, 2195–2211 (2021).
2. F. Ratjen *et al.*, Cystic fibrosis. *Nat. Rev. Dis. Primers* **1**, 15010 (2015).
3. I. Klein, B. Sarkadi, A. Váradi, An inventory of the human ABC proteins. *Biochim. Biophys. Acta* **1461**, 237–262 (1999).
4. M. J. Watson *et al.*, The cystic fibrosis transmembrane conductance regulator (CFTR) uses its C-terminus to regulate the A2B adenosine receptor. *Sci. Rep.* **6**, 27390 (2016).
5. F. A. L. Marson, C. S. Bertuzzo, J. D. Ribeiro, Classification of CFTR mutation classes. *The Lancet Respir. Med.* **4**, e37–e38 (2016).
6. K. Y. Jih, M. Li, T. C. Hwang, S. G. Bompadre, The most common cystic fibrosis-associated mutation destabilizes the dimeric state of the nucleotide-binding domains of CFTR. *J. Physiol.* **589**, 2719–2731 (2011).
7. J. Zielenski, L. C. Tsui, Cystic fibrosis: Genotypic and phenotypic variations. *Annu. Rev. Genet.* **29**, 777–807 (1995).
8. T. Okiyoneda *et al.*, Peripheral protein quality control removes unfolded CFTR from the plasma membrane. *Science* **329**, 805–810 (2010).
9. Y. Guo, M. Su, M. A. McNutt, J. Gu, Expression and distribution of cystic fibrosis transmembrane conductance regulator in neurons of the human brain. *J. Histochem. Cytochem.* **57**, 1113–1120 (2009).
10. J. Emerson, M. Rosenfeld, S. McNamara, B. Ramsey, R. L. Gibson, Pseudomonas aeruginosa and other predictors of mortality and morbidity in young children with cystic fibrosis. *Pediatr. Pulmonol.* **34**, 91–100 (2002).
11. C. Gangell *et al.*, Inflammatory responses to individual microorganisms in the lungs of children with cystic fibrosis. *Clin. Infect. Dis.* **53**, 425–432 (2011).
12. J. Adjemian, K. N. Olivier, D. R. Prevots, Nontuberculous mycobacteria among patients with cystic fibrosis in the United States: Screening practices and environmental risk. *Am. J. Respir Crit. Care Med.* **190**, 581–586 (2014).
13. K. Yoshimura *et al.*, Expression of the cystic fibrosis transmembrane conductance regulator gene in cells of non-epithelial origin. *Nucleic Acids Res.* **19**, 5417–5423 (1991).
14. H. H. Öz *et al.*, Recruited monocytes/macrophages drive pulmonary neutrophilic inflammation and irreversible lung tissue remodeling in cystic fibrosis. *Cell Rep.* **41**, 111797 (2022).
15. B. T. Kopp *et al.*, Exaggerated inflammatory responses mediated by Burkholderia cenocepacia in human macrophages derived from Cystic fibrosis patients. *Biochem. Biophys. Res. Commun.* **424**, 221–227 (2012).
16. P. D. Sly *et al.*, Risk factors for bronchiectasis in children with cystic fibrosis. *N. Engl. J. Med.* **368**, 1963–1970 (2013).
17. R. L. Young *et al.*, Neutrophil extracellular trap (NET)-mediated killing of Pseudomonas aeruginosa: Evidence of acquired resistance within the CF airway, independent of CFTR. *PLoS One* **6**, e23637 (2011).
18. E. M. Bruscia *et al.*, Abnormal trafficking and degradation of TLR4 underlie the elevated inflammatory response in cystic fibrosis. *J. Immunol.* **186**, 6990–6998 (2011).
19. S. Lara-Reyna *et al.*, Metabolic reprograming of cystic fibrosis macrophages via the IRE1α arm of the unfolded protein response results in exacerbated inflammation. *Front. Immunol.* **10**, 1789 (2019), 10.3389/fimmu.2019.01789.
20. K. Simonin-Le Jeune *et al.*, Impaired functions of macrophage from cystic fibrosis patients: CD11b, TLR-5 decrease and sCD14, Inflammatory Cytokines Increase. *PLOS One* **8**, e75667 (2013).
21. P. Del Porto *et al.*, Dysfunctional CFTR alters the bactericidal activity of human macrophages against Pseudomonas aeruginosa. *PLoS One* **6**, e19970 (2011).
22. A. A. Tarique *et al.*, CFTR-dependent defect in alternatively-activated macrophages in cystic fibrosis. *J. Cyst. Fibros.* **16**, 475–482 (2017).
23. H. H. Jarosz-Griffiths *et al.*, Different CFTR modulator combinations downregulate inflammation differently in cystic fibrosis. *Elife* **9**, e54556 (2020).
24. L. Cavinato *et al.*, Elexacaftor/tezacaftor/ivacaftor corrects monocyte microbicidal deficiency in cystic fibrosis. *Eur. Respir. J.* **61**, 2200725 (2023).
25. J. E. Payne *et al.*, Activity of innate antimicrobial peptides and ivacaftor against clinical cystic fibrosis respiratory pathogens. *Int. J. Antimicrob. Agents* **50**, 427–435 (2017).
26. A. T. Trimble, S. H. Donaldson, Ivacaftor withdrawal syndrome in cystic fibrosis patients with the G551D mutation. *J. Cyst. Fibros.* **17**, e13–e16 (2018).
27. C. J. Stocks, M. A. Schembri, M. J. Sweet, R. Kapetanovic, For when bacterial infections persist: Toll-like receptor-inducible direct antimicrobial pathways in macrophages. *J. Leukocyte Biol.* **103**, 35–51 (2018).
28. H. Botella *et al.*, Mycobacterial p(1)-type ATPases mediate resistance to zinc poisoning in human macrophages. *Cell Host Microbe* **10**, 248–259 (2011).
29. C. L. Ong, C. M. Gillen, T. C. Barnett, M. J. Walker, A. G. McEwan, An antimicrobial role for zinc in innate immune defense against group A streptococcus. *J. Infect. Dis.* **209**, 1500–1508 (2014).
30. R. Kapetanovic *et al.*, Salmonella employs multiple mechanisms to subvert the TLR-inducible zinc-mediated antimicrobial response of human macrophages. *Faseb J.* **30**, 1901–1912 (2016).
31. C. J. Stocks *et al.*, Uropathogenic Escherichia coliemploys both evasion and resistance to subvert innate immune-mediated zinc toxicity for dissemination. *Proc. Natl. Acad. Sci. U.S.A.* **116**, 6341–6350 (2019).
32. J. Jeong, D. J. Eide, The SLC39 family of zinc transporters. *Mol. Aspects Med.* **34**, 612–619 (2013).
33. D. Angyal, M. J. C. Bijvelds, M. J. Bruno, M. P. Peppelenbosch, H. R. de Jonge, Bicarbonate Transport in Cystic Fibrosis and Pancreatitis. *Cells* **11**, 54 (2021).
34. C. A. Cotrim *et al.*, Heterologous expression and biochemical characterization of the human zinc transporter 1 (ZnT1) and its soluble C-terminal domain. *Front. Chem.* **9**, 667803 (2021).
35. E. Shusterman *et al.*, ZnT-1 extrudes zinc from mammalian cells functioning as a Zn(2+)/H(+) exchanger. *Metallomics* **6**, 1656–1663 (2014).
36. L. Huang, S. Tepaamorndech, The SLC30 family of zinc transporters - a review of current understanding of their biological and pathophysiological roles. *Mol. Aspects Med.* **34**, 548–560 (2013).
37. A. Di *et al.*, CFTR regulates phagosome acidification in macrophages and alters bactericidal activity. *Nat. Cell Biol.* **8**, 933–944 (2006).
38. T. Ma *et al.*, Thiazolidinone CFTR inhibitor identified by high-throughput screening blocks cholera toxin–induced intestinal fluid secretion. *J. Clin. Invest.* **110**, 1651–1658 (2002).
39. S. Zhang, C. L. Shrestha, B. T. Kopp, Cystic fibrosis transmembrane conductance regulator (CFTR) modulators have differential effects on cystic fibrosis macrophage function. *Sci. Rep.* **8**, 17066 (2018).
40. N. K. Petty *et al.*, Global dissemination of a multidrug resistant Escherichia coli clone. *Proc. Natl. Acad. Sci. U.S.A.* **111**, 5694–5699 (2014).
41. R. Barnaby *et al.*, Lumacaftor (VX-809) restores the ability of CF macrophages to phagocytose and kill Pseudomonas aeruginosa. *Am. J. Physiol. Lung Cell Mol. Physiol.* **314**, L432–L438 (2018).
42. C. J. Stocks *et al.*, Frontline science: LPS-inducible SLC30A1 drives human macrophage-mediated zinc toxicity against intracellular Escherichia coli. *J. Leukocyte Biol.* **109**, 287–297 (2021).
43. S. J. Beard, R. Hashim, J. Membrillo-Hernández, M. N. Hughes, R. K. Poole, Zinc(II) tolerance in Escherichia coli K-12: Evidence that the zntA gene (o732) encodes a cation transport ATPase. *Mol. Microbiol.* **25**, 883–891 (1997).
44. C. Rensing, B. Mitra, B. P. Rosen, The zntA gene of Escherichia coli encodes a Zn(II)-translocating P-type ATPase. *Proc. Natl. Acad. Sci. U.S.A.* **94**, 14326–14331 (1997).
45. J. B. von Pein, C. J. Stocks, M. A. Schembri, R. Kapetanovic, M. J. Sweet, An alloy of zinc and innate immunity: Galvanising host defence against infection. *Cell Microbiol.* **23**, e13268 (2021).
46. T. Hussell, T. J. Bell, Alveolar macrophages: Plasticity in a tissue-specific context. *Nat. Rev. Immunol.* **14**, 81–93 (2014).
47. M. Kopf, C. Schneider, S. P. Nobs, The development and function of lung-resident macrophages and dendritic cells. *Nat. Immunol.* **16**, 36–44 (2015).
48. B. D. Chen, M. Mueller, T. H. Chou, Role of granulocyte/macrophage colony-stimulating factor in the regulation of murine alveolar macrophage proliferation and differentiation. *J. Immunol.* **141**, 139–144 (1988).
49. J. Gschwend *et al.*, Alveolar macrophages rely on GM-CSF from alveolar epithelial type 2 cells before and after birth. *J. Exp. Med.* **218**, e20210745 (2021).
50. G. Davies, A. U. Wells, S. Doffman, S. Watanabe, R. Wilson, The effect of Pseudomonas aeruginosa on pulmonary function in patients with bronchiectasis. *Euro. Respir. J.* **28**, 974–979 (2006).
51. M. Marguerettaz *et al.*, Sputum containing zinc enhances carbapenem resistance, biofilm formation and virulence of Pseudomonas aeruginosa. *Microb. Pathog.* **77**, 36–41 (2014).
52. J. H. Lee, Y. G. Kim, M. H. Cho, J. Lee, ZnO nanoparticles inhibit Pseudomonas aeruginosa biofilm formation and virulence factor production. *Microbiol. Res.* **169**, 888–896 (2014).
53. C. V. Prateeksha, A. K. Rao, S. K. Das, B. N. Barik, Singh, ZnO/Curcumin nanocomposites for enhanced inhibition of pseudomonas aeruginosa virulence via LasR-RhlR quorum sensing systems. *Mol. Pharm.* **16**, 3399–3413 (2019).
54. T. Ong, B. W. Ramsey, Cystic fibrosis: A review. *Jama* **329**, 1859–1871 (2023).
55. S. Sheikh *et al.*, Impact of elexacaftor-tezacaftor-ivacaftor on bacterial colonization and inflammatory responses in cystic fibrosis. *Pediatr. Pulmonol.* **58**, 825–833 (2023).
56. D. P. Nichols *et al.*, Pharmacologic improvement of CFTR function rapidly decreases sputum pathogen density, but lung infections generally persist. *J. Clin. Invest.* **133**, e167957 (2023).
57. E. M. Bruscia, T. L. Bonfield, Cystic fibrosis lung immunity: The role of the macrophage. *J. Innate Immun.* **8**, 550–563 (2016).
58. H. Gao, W. Dai, L. Zhao, J. Min, F. Wang, The role of zinc and zinc homeostasis in macrophage function. *J. Immunol. Res.* **2018**, 6872621 (2018).
59. X. Liu, M. K. Ali, K. Dua, R. Xu, The role of zinc in the pathogenesis of lung disease. *Nutrients* **14**, 2115 (2022).
60. I. Wessels, M. Maywald, L. Rink, Zinc as a gatekeeper of immune function. *Nutrients* **9**, 1286 (2017).
61. S. Bao, D. L. Knoell, Zinc modulates cytokine-induced lung epithelial cell barrier permeability. *Am. J. Physiol. Lung Cell Mol. Physiol.* **291**, L1132–L1141 (2006).

62. V. Damphousse, M. Mailhot, Y. Berthiaume, R. Rabasa-Lhoret, G. Mailhot, Plasma zinc in adults with cystic fibrosis: Correlations with clinical outcomes. *J. Trace Elem. Med. Biol.* **28**, 60–64 (2014).
63. S. E. Bauer *et al.*, Zinc status and growth in infants and young children with cystic fibrosis. *Pediatr. Pulmonol.* **56**, 3768–3776 (2021).
64. L. Akanli, D. B. Lowenthal, S. Gjonaj, A. J. Dozor, Plasma and red blood cell zinc in cystic fibrosis. *Pediatr. Pulmonol.* **35**, 2–7 (2003).
65. A. AbdulWahab *et al.*, Serum zinc concentration in cystic fibrosis patients with CFTR I1234V mutation associated with pancreatic sufficiency. *Clin. Respir. J.* **11**, 305–310 (2017).
66. J. P. Liuzzi *et al.*, Interleukin-6 regulates the zinc transporter Zip14 in liver and contributes to the hypozincemia of the acute-phase response. *Proc. Natl. Acad. Sci. U.S.A.* **102**, 6843–6848 (2005).
67. B. A. Eijkelkamp *et al.*, Dietary zinc and the control of Streptococcus pneumoniae infection. *PLoS Pathog.* **15**, e1007957 (2019).
68. S. Kamei *et al.*, Zinc deficiency via a splice switch in zinc importer ZIP2/SLC39A2 causes cystic fibrosis-associated MUC5AC hypersecretion in airway epithelial cells. *EBioMedicine* **27**, 304–316 (2018).
69. E. Garay *et al.*, Tryptophan regulates Drosophila zinc stores. *Proc. Natl. Acad. Sci. U.S.A.* **119**, e2117807119 (2022).
70. P. Kondaiah, P. S. Yaduvanshi, P. A. Sharp, R. Pullakhandam, Iron and zinc homeostasis and interactions: Does enteric zinc excretion cross-talk with intestinal iron absorption? *Nutrients* **11**, 1885 (2019).
71. H. F. Hazlett *et al.*, Altered iron metabolism in cystic fibrosis macrophages: The impact of CFTR modulators and implications for Pseudomonas aeruginosa survival. *Sci. Rep.* **10**, 10935 (2020).
72. C. Lang *et al.*, Anti-inflammatory effects of zinc and alterations in zinc transporter mRNA in mouse models of allergic inflammation. *Am J. Physiol. Lung Cell Mol. Physiol.* **292**, L577–L584 (2007).
73. N. F. Krebs *et al.*, Abnormalities in zinc homeostasis in young infants with cystic fibrosis. *Pediatr. Res.* **48**, 256–261 (2000).
74. I. Abdulhamid, F. W. Beck, S. Millard, X. Chen, A. Prasad, Effect of zinc supplementation on respiratory tract infections in children with cystic fibrosis. *Pediatr. Pulmonol.* **43**, 281–287 (2008).
75. G. Sharma *et al.*, Zinc supplementation for one year among children with cystic fibrosis does not decrease pulmonary infection. *Respir. Care* **61**, 78–84 (2016).
76. L. Fuortes, D. Schenck, Marked elevation of urinary zinc levels and pleural-friction rub in metal fume fever. *Vet. Hum. Toxicol.* **42**, 164–165 (2000).
77. K. McBride, B. Slotnick, F. L. Margolis, Does intranasal application of zinc sulfate produce anosmia in the mouse? An olfactometric and anatomical study. *Chem. Senses* **28**, 659–670 (2003).
78. I. Pagan, D. L. Costa, J. K. McGee, J. H. Richards, J. A. Dye, Metals mimic airway epithelial injury induced by in vitro exposure to Utah Valley ambient particulate matter extracts. *J. Toxicol. Environ. Health A* **66**, 1087–1112 (2003).
79. S. H. Gavett, N. Haykal-Coates, L. B. Copeland, J. Heinrich, M. I. Gilmour, Metal composition of ambient PM2.5 influences severity of allergic airways disease in mice. *Environ. Health Perspect.* **111**, 1471–1477 (2003).
80. L. Bohlmann *et al.*, Chemical synergy between ionophore PBT2 and zinc reverses antibiotic resistance. *mBio* **9**, e02391-18 (2018).
81. D. M. P. De Oliveira *et al.*, Repurposing a neurodegenerative disease drug to treat Gram-negative antibiotic-resistant bacterial sepsis. *Sci. Transl. Med.* **12**, eabb3791 (2020).
82. P. J. Barry *et al.*, Triple therapy for cystic fibrosis Phe508del-gating and -residual function genotypes. *N. Engl. J. Med.* **385**, 815–825 (2021).
83. D. P. Nichols *et al.*, Clinical effectiveness of elexacaftor/tezacaftor/ivacaftor in people with cystic fibrosis: A clinical trial. *Am. J. Respir Crit. Care Med.* **205**, 529–539 (2022).
84. H. G. M. Heijerman *et al.*, Efficacy and safety of the elexacaftor plus tezacaftor plus ivacaftor combination regimen in people with cystic fibrosis homozygous for the F508del mutation: A double-blind, randomised, phase 3 trial. *Lancet* **394**, 1940–1948 (2019).
85. P. G. Middleton *et al.*, Elexacaftor-tezacaftor–ivacaftor for cystic fibrosis with a single Phe508del allele. *N. Engl. J. Med.* **381**, 1809–1819 (2019).
86. N. Volkova *et al.*, Disease progression in patients with cystic fibrosis treated with ivacaftor: Data from national US and UK registries. *J. Cyst. Fibros.* **19**, 68–79 (2020).
87. K. B. Hisert *et al.*, Restoring cystic fibrosis transmembrane conductance regulator function reduces airway bacteria and inflammation in people with cystic fibrosis and chronic lung infections. *Am. J. Respir. Crit. Care Med.* **195**, 1617–1628 (2017).
88. J. K. Harris *et al.*, Changes in airway microbiome and inflammation with ivacaftor treatment in patients with cystic fibrosis and the G551D mutation. *Ann. Am. Thorac. Soc.* **17**, 212–220 (2020).
89. B. C. Millar, J. McCaughan, J. C. Rendall, D. G. Downey, J. E. Moore, Pseudomonas aeruginosa in cystic fibrosis patients with c.1652G>A (G551D)-CFTR treated with ivacaftor–Changes in microbiological parameters. *J. Clin. Pharm. Ther.* **43**, 92–100 (2018).
90. S. Zhang *et al.*, Cystic fibrosis macrophage function and clinical outcomes after elexacaftor/tezacaftor/ivacaftor. *Euro. Respir. J.* **61**, 2102861 (2022).
91. S. G. Bompadre, Y. Sohma, M. Li, T. C. Hwang, G551D and G1349D, two CF-associated mutations in the signature sequences of CFTR, exhibit distinct gating defects. *J. Gen. Physiol.* **129**, 285–298 (2007).
92. F. Becq *et al.*, The rescue of F508del-CFTR by elexacaftor/tezacaftor/ivacaftor (Trikafta) in human airway epithelial cells is underestimated due to the presence of ivacaftor. *Eur. Respir. J.* **59**, 2100671 (2022).
93. F. R. Blattner *et al.*, The complete genome sequence of Escherichia coli K-12. *Science* **277**, 1453–1462 (1997).
94. K. Das Gupta *et al.*, HDAC7 is an immunometabolic switch triaging danger signals for engagement of antimicrobial versus inflammatory responses in macrophages. *Proc. Natl. Acad. Sci. U.S.A.* **120**, e2212813120 (2023).
95. M. Totsika *et al.*, Insights into a multidrug resistant Escherichia coli pathogen of the globally disseminated ST131 lineage: Genome analysis and virulence mechanisms. *PloS One* **6**, e26578 (2011).
96. M. W. Tan, S. Mahajan-Miklos, F. M. Ausubel, Killing of Caenorhabditis elegans by Pseudomonas aeruginosa used to model mammalian bacterial pathogenesis. *Proc. Natl. Acad. Sci. U.S.A.* **96**, 715–720 (1999).
97. N. J. Bokil *et al.*, Intramacrophage survival of uropathogenic Escherichia coli: Differences between diverse clinical isolates and between mouse and human macrophages. *Immunobiology* **216**, 1164–1171 (2011).
98. K. J. Livak, T. D. Schmittgen, Analysis of relative gene expression data using real-time quantitative PCR and the 2(-Delta Delta C(T)) Method. *Methods* **25**, 402–408 (2001).